EasyChair Preprint

№ 7751

wPLI for Pre-Training Desynchronization Identification

F.Y. Zapata, O.W. Gómez, A.M. Alvarez and C.G. Castellanos

April 10, 2022

wPLI for Pre-training desynchronization Identification

Abstract. Motor processing can result in coordinated changes of ongoing/decreasing brain neural activity, or event-related de/synchronization (ERD/S), over both lateral brain hemispheres. Because of Motor processing can result in coordinated changes of ongoing/decreasing brain neural activity, or event-related de/synchronization (ERD/S), over both lateral brain hemispheres. Because of the affordability and time resolution provided, Electroencephalographic (EEG) signals are commonly used to acquire motor imagery paradigms. However, the widely known condition of low-noise signals makes detection and spatial localization of ERD/S challenging. Here, to deal with the high variability between subjects, we propose to perform group analysis of graph representations extracted from the weighted Phase lock Index. Statistical thresholding of the functional connectivity estimates is also accomplished to improve the assessments of phase synchronization between electrodes. The obtained results on a real-world database with 50 individuals show that the proposed methodology improves interpretation of ERD/S, allowing better prediction of motor imagery ability in subjects having low skills for practicing this paradigm.

Keywords: Event-related Synchronization/Desynchronization, Functional Connectivity, Group analysis, wPLI.

1 Introduction

Motor imagery (MI) is a dynamic mental state in which an individual performs a mental rehearsal of motor action without any overt output. It is believed that actual movements and those performed mentally (imaginary movements) are functionally similar [1]. Therefore, there is sufficient experimental evidence that MI contributes to substantial improvements in motor learning and performance [2], games and entertainment, sports training, therapy to induce recovery and neuroplasticity in neurophysical regulation and rehabilitation, and activation of brain neural networks as the basis of motor learning [3], and education scenarios [4]. These applications reinforce the importance of studying the evolving brain organization to model plastic changes accurately, putting strength on dynamic modeling of temporal, spectral, and spatial features extracted from single channels since most MI systems rely on them to distinguish distinctive neural activation patterns [5].

MI systems handle brain data recorded with electroencephalography (EEG), which is a noninvasive measurement of neural activation and interactions, encoding brain dynamics with high temporal granularity, but at a relatively low spatial resolution [6]. Also, Functional Connectivity (FC) networks are extracted because a better understanding of MI mechanisms requires knowledge of the way the co-activated brain regions interact with each other [7]. Another characterizing the imaged hand

movements is to quantify frequency alterations in time-varying responses to a stimulus (event) through the so-termed Event-Related De/Synchronization (ERD/S), presenting a significant correlate of localized cortical oscillatory activity [8]. When imagining one hand moving, an increase/decrease in the power of μ and β rhythms becomes more potent in the sensorimotor (electrodes C_3 and C_4) and premotor (C_z) areas located contralaterally to the hand involved in the task [9]. However, due to the non-stationarity of EEG data, the effectiveness of feature extraction procedures is reduced in deriving distinct EEG spatio-spectral patterns. Several factors can affect, among others, the following: movement artifacts during recording, temporal stability of mirroring activation over several sessions differs notably between MI time intervals [10], low EEG signal-to-noise ratio, poor performance in small-sample settings [11], and inter-subject variability in EEG dynamics [12]. Along with variability in the signal acquisition, another circumstance that leads to low accuracy scores is that some subjects may have brain networks not sufficiently developed for practicing MI tasks [13]. As a result, the performance of MI systems varies considerably across and within subjects, severely degrading their reliability.

Here, we develop a dynamic model for estimating the mutual neural activity across subjects to provide new insights into the evolution of collective mental imagery processes. The obtained validation results indicate that the estimated collective dynamics reflect the flow differently in the sensorimotor cortex. Therefore, the common model individually addresses inter-subject and inter-trial variability sources, depending on the engaged extraction method.

2 Methods and Experimental Setup

Ensemble-based Weighted Phase Locking Index (wPLI): is commonly used to estimate functional connectivity and quantifies the asymmetry of phase difference distribution between two specific channels due to its nonparametric nature and easy implementation:

$$v\,(c, c')=| \mathrm{E}\{\mathscr{F}\{ S(c, c'; n, f)\}: \forall n \in N\}|/ \mathrm{E}\{|\mathscr{F}\{ S(c, c'; n, f): \forall n \in N\}|\},\ v(,) \in [0,1] \quad (1)$$

where $S(c, c'; n, f) \in \mathbb{C}$ is the cross-spectral density based on Morlet wavelets and $\mathscr{F}\{.\}$ stands for the imaginary part of a complex-valued function, $\mathrm{E}\{.\}$ average of all trials with $c \in C$.
Besides, the following weighted network indexes are extracted from either phase synchronization measures:

Strength is a local-scale property that accounts for the number of links connected to each node, computed as follows:

$$\varphi_1(c) = C\,\mathrm{E}\{v(c, c') : \forall c' \in C, c' \neq c\} \quad (2)$$

For evaluation purposes, we use the pipeline of the supervised piecewise network connectivity analysis, appraising two stages.

2.1 MI Databases Description and Pre-processing

Gigadb: We explore the collection publicly available at[1] that holds EEG data obtained from fifty-two subjects (although only M = 50 are available) using a 10-10 placement electrode system with C=64 channels. Each channel x(c) lasted T = 7*s*, and was sampled at Fs = 512 *Hz*. At the beginning of the test, a fixation cross was displayed on a black screen during 2*s*. Then, linked to either MI label \lambda= l or \lambda = l', a cue instruction appeared randomly on the screen within 3*s*. The cue asked each subject to imagine moving his fingers, starting to form the index finger and reaching the little finger, and touching each to his thumb. A blank screen was then displayed at the beginning of a break period, which ran randomly between 4.1 and 4.8 *s*. In addition, a single-trial resting-state recording, lasting 60*s*, was collected from each subject.

Every raw EEG channel of either database was band-pass filtered in the frequency range $f \in$ [4-40] *Hz*, covering the sensorimotor rhythms considered (μ, β). Then, the band-passed EGG data are spatially filtered by a Laplacian filter centered on the selected electrode.

3 Results

3.1 Subject-level Graph Connectivity Extraction

Initially, a key parameter to fix is the window length to extract the functional connectivity measures considered. Analyzing the mean and standard deviation of accuracy 87.2±11.6, averaged across the subject set, indicates that the length of τ=2*s* present more separability, for MI in $\Delta T_3 \in$ [2.5-4.5] *s* and in resting-state with 30 trials ΔT, can be considered a convenient trade-off between accuracy and the number of samples to be processed.

The following parameter to adjust is the connection threshold *q*, a widely used functional connectivity analysis technique to remove false connections and noise. Empirically, we found that the best values for q=0.7 can be selected as a comprise value that preserves a sufficient amount of links below $p<0.05$.

3.2 Extraction Clustering of intra/inter-subject variability

To consider the influence of BCI Inefficiency, we cluster the diversity in intra/inter-subject variability to obtain subject partitions with related levels of variability in brain neural responses. For comparison purposes, we examine three strategies to infer the

[1] http://gigadb.org/dataset/100295

distinctiveness between a fixed number of subject partitions: i) Baseline consideration a group with SMR and accuracy [14,15], ii) Group based on force graph Strength.

i) *Grouping based on accuracy response and neural indicators.* We perform clustering of groups with a similar variability behavior under the assumption that the more accurate the subject in distinguishing between MI tasks, the more efficient the individual brain network, as evidenced in [14]. To estimate the number of partitions, as suggested in [16], we feed the *k*-means algorithm with the accuracy sets accounting for the performance variability because of different evaluated extraction window lengths and the indicator values of neural desynchronization at rest over the sensorimotor area. After adjusting the cluster inertia by the Silhouette score, the number of partitions turns out to be three. For the dataset evaluated, the top row in Figure 1(a) presents the resulting clustering drawn in color bars: G1 holds the subjects performing the best (green color), G2 with the middle-performance (yellow color), G3 with the worst-performing individuals (red color). Although either database provides partitions with a low overlapping ratio, the groups also follow the accuracy rank appropriately. As a result, the subjects are not intertwined, as seen in the middle row.

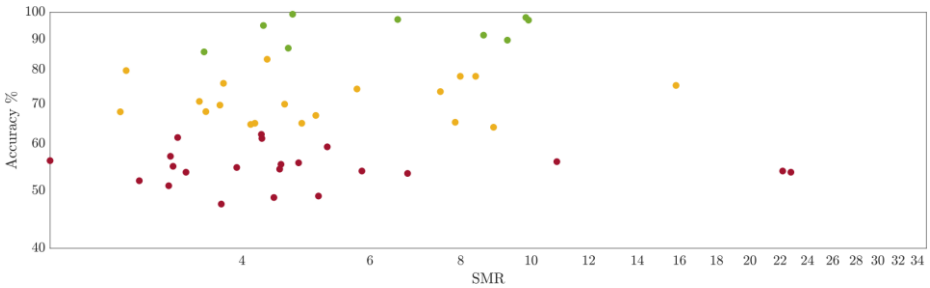

[a] Clustering

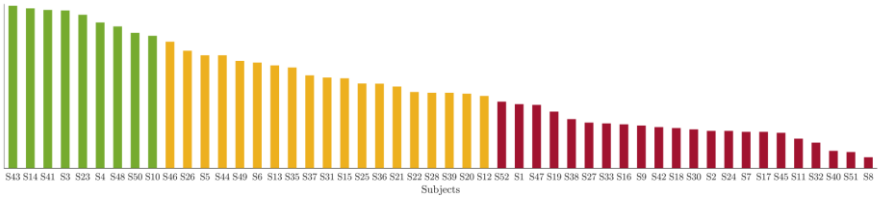

[b] Ranked subject accuracy of DI

Fig. 1. Subject clustering using correlates between accuracy and power-based indicators extracted from sensorimotor rhythms.

ii) Subject clustering by Graphs. After calculating the wPLI connectivity and performing the Strength graph measurements, we perform groupings and identify the internal behavior between MI tasks. The top row in Figure 2(a - b) presents the resulting grouping in colored bars, where G1 contains the subjects that show better performance compared to the graph measures (Green color), G2 includes the average version (yellow), G3 with individuals with low performance (Red color). Taking into account

the analysis in Figure 2(a), we do the grouping taking into account all the connections. For Figure 2(b) we only take into account the connections of the motor region, which allows me to identify the change in G1 and G2 that is evidenced in Figure 2(c - d), where there is an increase in subjects from G1 compared to G2.

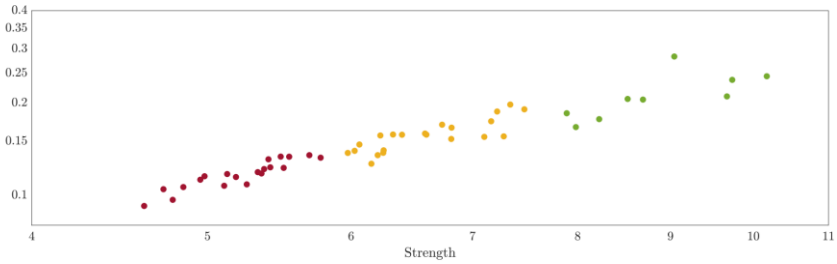

(a) Partitions clustering all channels

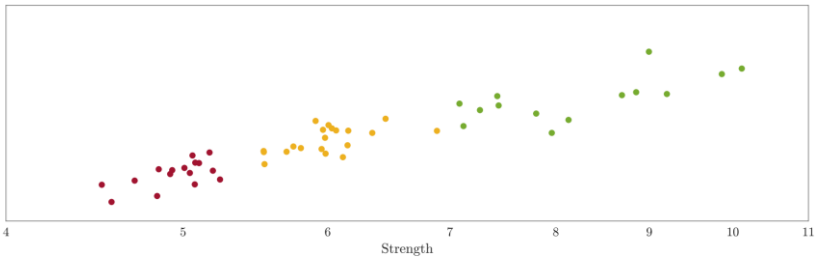

(b) partitions clustering center channels

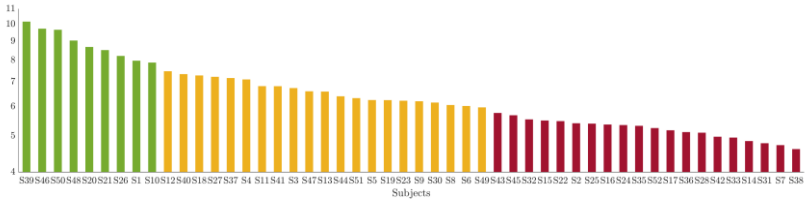

(c) All channels

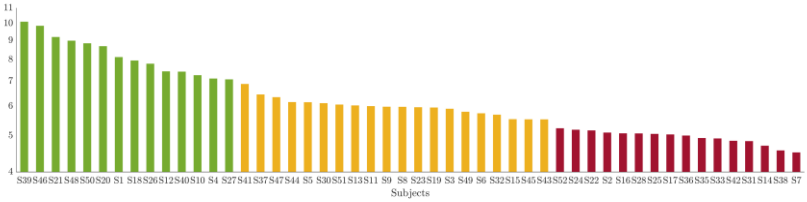

(d) Center channels

Fig. 2. Clustering through graph measures.

The difference in activity is evident following the behavior in the rest-state and the power of the channels C_3 and C_4.

Direct subject partition of pre-training desynchronization indicators

Table 1. Metric between (μ y β), activity in MI and Resting-state.

	All subjects		G1			G2		G3	
	r	p	r	P		r	p	r	p
	Strength								
C_3-C_4	0.410	0.003	0.099	0.658		0.548	0.126	**0.450**	0.053
SMR	0.261	0.066	0.189	0.399		**0.597**	0.088	0.343	0.150
All channels	0.141	0.040	**0.440**	0.040		0.227	0.555	0.265	0.271
	Strength vs Acc								
C_3-C_4	0.334	0.017	0.311	0.323		0.016	0.947	0.340	0.154
SMR	**0.556**	0.001	0.223	0.484		0.102	0.676	0.237	0.328
All channels	0.178	0.215	0.260	0.413		0.136	0.578	0.088	0.718

In Table 1, there is the estimation of all the subjects and for each of the groups, the calculation of the correlation and the p-value between the channels for the measurements, performing the analysis with variance in the configuration of the channels with the measure of Strength and accuracy that is displayed in Figure 1, where the most significant relationship is found in G1 with all the channels, for G2 in the SMR activity and G3 with the central channels, generating a relationship of common activity between the subjects, taking into account that the best configuration with SMR, related to the resting state, presents an activity between Strength and accuracy with higher correlation.

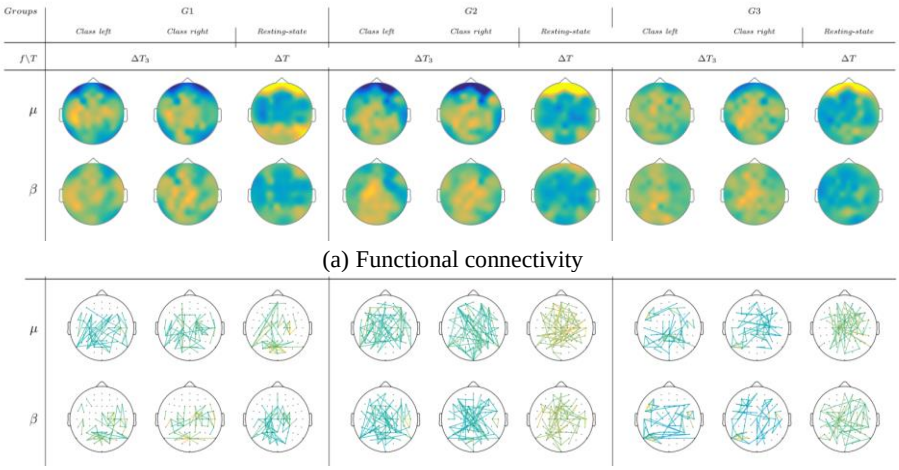

(a) Functional connectivity

(b) Brain connectivity network functional

Fig. 3. (a) In the window of motor imagination for the windows of the subjects selected from each of the groups by accuracy, (b) Three representative individuals performed by node strength, and extracted within the interval ΔT.

Visual inspection of FC activity for this group see Figure 3(a), it can be found that the connections of the areas associated (frontoparietal, central, parietal-occipital, temporal) with tasks such as (information processing, analysis, memory, concentration, sensorimotor zone) which was also found in [17].

From the above, it is evident that when analyzing the two databases, for each grouping mentioned above, similar areas are presented, such as the parietal, motor, and frontoparietal; this is generated by the results of connectivity when looking at integration as segregation, information that reveals the behavior of brain regions in the presence of tasks in motor imagination as seen in Figure 3(a). Lastly, it is crucial to remember that the grouping carried out exclusively by the success in classification allows separating the subjects according to their performance. Still, it does not guarantee an appropriate physiological interpretation since the zones with the most significant activation are found in the (areas somatosensory) of the head [18].

The second grouping strategy that takes into account the measures of the group (i.e., Strenght) shows that the separability between the connections of the groups is clear according to Figure 2. Besides, the brain activity in Figure 3(a) highlights the connections of the areas (frontoparietal, central, parietal-occipital, temporal) associated with tasks such as (sensorimotor zone, memory, concentration, information processing), which also is found in the works developed by [19]. As suggested in [20], the best physiological interpretability for the task analyzed in this exercise is related to motor imagination, including the state of rest, this presents activation in the sensory and motor areas (coincidence with analysis of the graphs). Therefore, the group analysis should be performed on time while preserving physiological interpretability.

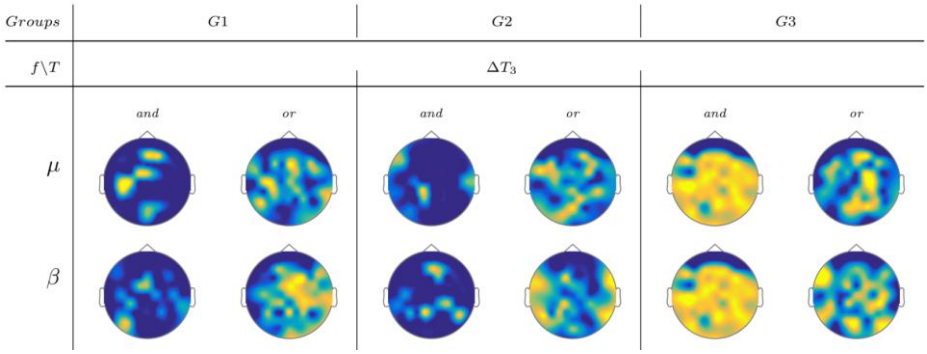

Fig. 4. The test between the classes to identify the connections that are relevant in the groups selected by graphs Strength, in the bands μ and β.

Figure 4 shows the behavior of the groups in each graph measurement, identifying the connectivity dynamics with spatial differences. At the group level, the activity reflected after estimating the strength measure results in low interaction of the groups with good performance G1 compared to the subjects with lower performance [21].
Therefore, their dynamics are related to connections with more information in the central-parietal zone. In group G3, one can see dynamics distributed over the entire surface. However, the G1 shows a higher clustering behavior in the μ band than the other groups.

Table 2. Measurements and average accuracy between groups.

	Acc			Metrics				
	G1	G2	G3	Silhouette	Mutual information	Rand Score	Homogeneity	Similarity
wPLI	71,90	74,78	69,01	0,22	0,47	0,47	0,47	0,44
wPLI+ Acc	58,62	88,57	64,72	0,21				
φ_1	81,00	72,14	71,91	0,57	0,91	0,91	0,93	0,96
φ_{1+Acc}	81,13	77,14	66,65	0,42				

As presented in Table 2, the Silhouette measurement identifies the best grouping strategy, though other grouping measures are also compared.

4 Concluding remarks

In summary, the need to make a grouping that highlights physiological interpretability is evident, and a good strategy is to take advantage of connectivities and graph analysis. In the results obtained in Table 2, it is evident that despite the quality of the clustering carried out, the high variability of the subjects, the heterogeneity of the connectivities, as well as the chosen threshold notably affect the activity that will be finally analyzed.

From the above, it is evident that when analyzing the two databases, for each grouping mentioned above, similar areas are presented, such as the parietal, motor, and frontoparietal; this is generated by the results of connectivity when looking at integration as segregation, information that reveals the behavior of brain regions in the presence of tasks in motor imagination as seen in Figure 3(a) and at the link level in Figure 3(b). In addition, Figure 3(b) displays the behaviors of the connectivity and correlation, indicating their homogeneity between subjects Resting State, as reported in [22].

It should be noted that using the same thresholding and same process conditions, there is less variability, preserving more compact areas of activity related to the principles of neuronal integration and segregation according to appointment [23,24]. Finally, from the graph measurements in Figure 3(b), it follows that the activity within the motor imagination window has the meaning of the connectivity response as also suggested in

[25]. It is feasible to use connectivity utils the graph properties as input supervised and unsupervised learning so that interpretability preserved improves results in both cases.

References

1. Stolbkov Y K, Moshonkina T R, Orlov I V, Tomilovskaya E S, Kozlovskaya I B and Gerasimenko Y P Human Physiology 45 104–114 (2019).
2. Aymeric G and Ursula D. Frontiers in Physiology 396 (2019).
3. Machado T C, Carregosa A A, Santos M S, da Silva Ribeiro N M and Melo A, Topics in Stroke Rehabilitation 0 1–6 (2019).
4. MacIntyre T, Madan C M A, Collet C and Guillot A, 240 141–159 (2018).
5. Hamedi M, Salleh S H and Noor A M, Neural Computation 28 999–1041 (2016).
6. Feng J, Jin J, Daly I, Zhou J, Niu Y, Wang X and Cichocki A, An optimized channel selection method based on multifrequency CSP-rank for motor imagery-based BCI system Comp. Int. and Neurosc (2019).
7. Stavrinou M L, Moraru L, Cimponeriu L, Della Penna S and Bezerianos A, Brain Topography 19 137–145 (2007).
8. Juan B, Santiago E, Arturo B M, Marius N, Javier B, Eduardo F, Surjo S and Nicolas G A, International journal of neural systems 29 1850045 (2019).
9. Wierzga la P, Zapala D, Wojcik G M and Masiak J, Frontiers in Neuroinformatics 12 78 (2018).
10. Pattnaik P K and Sarraf J, Computer and Information Sciences 30 18–24 (2018).
11. Park Y and Chung W IEEE Transactions on Neural Systems and Rehabilitation Engineering 27 1378–1388 (2019).
12. Saha S, Ahmed K I U, Mostafa R, Hadjileontiadis L and Khandoker A IEEE Transactions on Neural Systems and Rehabilitation Engineering 26 371–382 (2018).
13. Ahn M and Jun S C, Journal of neuroscience methods 243 103–110 (2015).
14. Blankertz B, Sannelli C, Halder S, Hammer E M, K¨ubler A, M¨uller K R, Curio G and Dickhaus T, Neuroimage 51 1303–1309 (2010).
15. Hammer E M, Halder S, Blankertz B, Sannelli C, Dickhaus T, Kleih S, M¨uller K R and K¨ubler A, Biological psychology 89 80–86 (2012).
16. Velasquez-Martinez L, Caicedo-Acosta J and Castellanos-Dominguez G, Entropy 22 703 (2020).
17. Rodrigues P G, Attux R, Castellano G, Soriano D C et al., Medical & biological engineering & computing 57 1709–1725 (2019).
18. Iwatsuki K, Hoshiyama M, Oyama S, Yoneda H, Shimoda S and Hirata H, Frontiers in Synaptic Neuroscience 12 7 (2020).
19. Sun S, Li X, Zhu J, Wang Y, La R, Zhang X, Wei L and Hu B, IEEE Transactions on Neural Systems and Rehabilitation Engineering 27 429–439 (2019).
20. Sareen E, Singh L, Gupta A, Verma R, Achary G K and Varkey B, IEEE Transactions on Neural Systems and Rehabilitation Engineering 28 2420–2430 (2020).
21. Kim Y K, Park E, Lee A, Im C H and Kim Y H, PLoS One 13 e0190715 (2018).
22. Vecchio F, Miraglia F, Quaranta D, Granata G, Romanello R, Marra C, Bramanti P and Rossini P M, Neuroscience 316 143–150 (2016).
23. Sporns O, Scholarpedia 2 4695 (2007)
24. Sporns O, Dialogues in Clinical Neuroscience 20 111 (2018).

Iyer P M, Egan C, Pinto-Grau M, Burke T, Elamin M, Nasseroleslami B, Pender N, Lalor E C and Hardiman O 2015 PloS one 10 e0128682 (2015).